Input–Output Selection for Planar Tensegrity Models

Bram de Jager and Robert E. Skelton

***Abstract*—The input–output selection approach followed in this brief uses a rigorous and systematic procedure, efficiently selecting actuators and/or sensors that guarantee a desired level of performance, embedded in a heuristic. The procedure generates all so-called minimal dependent sets and uses a closed-loop criterion. The heuristic is a divide-and-conquer one. This approach is applied to controlled tensegrity structures, using as criterion efficiently computable conditions for the existence of a stabilizing $\mathcal{H}_\infty$ controller achieving a desired level of performance. Structural systems, like controlled tensegrities, are a prime example for application of techniques that address system design issues, because they present opportunities in choosing actuators/sensors and in choosing their mechanical structure. Results for a three-unit planar tensegrity structure, where all 26 tendons can be used as actuator or sensor devices, making up 52 devices from which to choose, demonstrate the approach. Two design specifications were explored, one is related to the dynamical stiffness of the structure, the other to vibration isolation. The feasible sets of actuators and sensors depend on the specifications and really differ for both, but are mostly composed of much less than 52 devices.**

***Index Terms*—Flexible structures, $\mathcal{H}_\infty$ control, input–output selection, intelligent structures, optimization methods, structural control, tensegrity structures, vibration control.**

I. Introduction

THE ULTIMATELY achievable performance of a controlled plant depends on plant characteristics, on controller architecture, and on controller parameters. Normally plant and controller are designed separately, which may lead to a suboptimal performance of the closed loop. An integrated design, concurrently designing plant and control, is therefore important [1]. Sensors and actuators define the interface between plant and controller and, thus, require special attention in an integrated design.

This brief addresses the choice of type, number, and placement of actuation and sensing devices, or, more generally, of input and output signals used for the closed loop. Inappropriate selection of sensors may, for instance, lead to zeros in the right-half plane, a well known performance limiting factor. Other performance limiting factors are a high relative degree, disturbance and model error inputs that are not matched with control inputs, measurements that are not matched with performance related outputs, and a large model uncertainty near crossover. To avoid those factors, one aims at selecting an appropriate controller structure, e.g., those input–output devices for which a controller exists that will deliver a desired level of performance, which will exclude combinations with performance limitations. Besides performance, considerations like complexity and cost, e.g., number of devices, could also be considered in the selection.

A prime application of integrated design is tensegrity structures. These are truss-like mechanical structures that consist of two types of members, tensile (tendons) and compressive (bars), and that allow a state of self-stress [2]. Tensegrities are used as landmarks [3], as cell models [4], as engineering structures [5], and others. The integrity (stability) of a tensegrity structure is due to the tensile forces in the tendons, hence, the name *tensegrity*.

Actuating members improves stiffness, stiffness-to-mass, and damping properties, and allows shape changes. Sensing provides information about the (deformed) geometry of the structure. Actuation can be done by different means, for instance with:

- electroplastics or piezos, which change length under influence of an electric field;
- shape memory alloys, which change length under influence of a temperature field;
- telescopic bars [5];
- tendon rest-length changes, by hauling them with linear or rotary motors [6].

Here we consider only the tendons as members that can sense their own length and can change that length. Target areas of application for engineering tensegrity structures are when disturbances need to be rejected, when the shape of a structure needs to be changed dynamically, e.g., adaptive structures [5] and deployable space structures [7], [8].

Due to the large number of possibilities to assign actuators and sensors, tensegrity structures need an efficient approach for input–output selection. Solutions to input–output selection are abundant [9]. Input–output selection targeted at engineering structures, e.g., [10]–[19], is normally characterized by one or more of the following restrictions:

- consideration of actuators *or* sensors *or* collocated pairs;
- enumeration of a limited set of candidates;
- consideration of location, not location and number, of devices;
- approximate solution (e.g., by stochastic search);
- selection criteria that only approximate closed-loop performance

to overcome computational problems. We want to get away from these restrictions, while still solving problems that are relevant for engineering practice, i.e., large ones. Selection of the devices or signals based on a full candidate-by-candidate feasibility test is a combinatorial problem. The selection can be simplified by

Manuscript received September 25, 2003. Manuscript received in final form February 2, 2005. Recommended by Associate Editor K. Kozlowski.

B. de Jager is with the Department of Mechanical Engineering, Technische Universiteit Eindhoven, 5600 MB Eindhoven, The Netherlands (e-mail: A.G.de.Jager@wfw.wtb.tue.nl).

B. Skelton is with the Department of Mechanical and Aerospace Engineering, University of California at San Diego, La Jolla, CA 92093 USA (e-mail: bobskelton@ucsd.edu) www.mae.ucsd.edu/research/reskelton/laboratory/SSCL.htm.

Digital Object Identifier 10.1109/TCST.2005.847346

not using a candidate-by-candidate test, often only with a crude selection criterion or with an approximate solution, making it likely to be less effective because favorable combinations of actuators and sensors can be missed. Finding a good approach for input–output selection is like a balancing act. Aiming at generality and rigor makes it quite hard to find a solution, and therefore hardly practical for large systems. Making it easy to find an answer may lead to sloppy results.

In [20], we applied a procedure that is more refined than brute force. The selection is still based on a candidate-by-candidate like test. It uses a streamlined rigorous feasibility test combined with an efficient search, subject to a mild assumption. Larger problems may then be tackled in acceptable time, because only a limited number of combinations needs to be tested. Although with this procedure the problem is theoretically still combinatorial in the number of devices, in practice the complexity is affine in the number of inputs and outputs and in the size of the solution. This is still not sufficiently efficient for problems that arise in practice. Therefore, here this procedure is combined with a heuristic to make it applicable for large scale problems.

We consider a three-unit planar tensegrity structure with 26 tendons and two different closed-loop specifications. Suppose, from the 52 admissible devices, only 32 devices are allowed to be treated simultaneously. To accommodate this, the heuristic used was to split up the selection in three steps. First selecting actuators, assuming all sensors to be used. Then selecting sensors, assuming all actuators to be used. From the most promising results of these selections, a set of 32 devices is selected to find solutions with a lower number of devices that still meet the required performance level. This is performed for several performance levels, to get insight in the relation between the number of devices and the achievable performance, and for both design specifications.

The goal of the brief is to address the problem of efficient and effective input–output selection for integrated design problems, as outlined previously, and apply the techniques on tensegrity systems, although they can be applied to other systems, e.g., chemical plants, noise control, as well. The main contributions are the integration of a rigorous actuator/sensor selection procedure with a heuristic, for which it is still likely that the results are rigorous, circumventing all restrictions outlined previously, and the presentation of a convincing example of this property.

The brief is structured as follows. First, we discuss tensegrity structures and a nonlinear dynamic model of planar tensegrity. Then we present the linearized model, the control design, and the feasibility test, followed by an explanation of the search. An application for a planar tensegrity shows the approach applied to a large scale selection problem. A conclusion finishes the brief.

II. Planar Tensegrity Structures

A tensegrity structure consists of bars and tendons, arranged in such a way that the structure has integrity and is not a mechanism. This is achieved by self-stressing the tendons by a tensile force. A planar tensegrity structure is one that only extends in the plane.

An elementary unit, numbered i, of a planar tensegrity structure is given in Fig. 1. This unit can be repeated indefinitely,

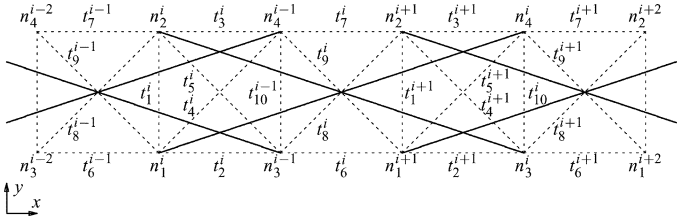

Fig. 1. Single unit of planar tensegrity structure. Bars: ——. Tendons: — —.

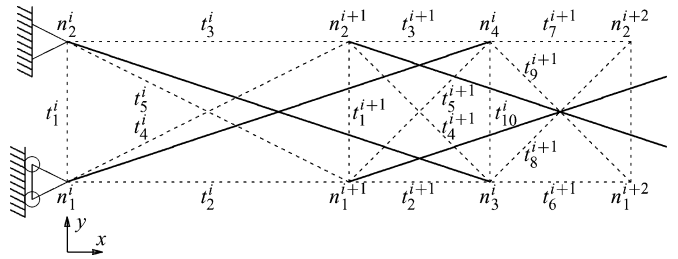

Fig. 2. Left unit of planar tensegrity structure $i = 1$.

by replicating it, shifted some distance of the horizontal dimension, to build up a planar structure in x-direction. It could also be replicated in y-direction or both. Indicated are the numbering of the tendons that belong to unit i, given by t_α^i, with $1 \leq \alpha \leq 10$. Also indicated are tendons of units $i-1$ and $i+1$ that are connected to the four endpoints (nodes) n_{1-4}^i of the two bars of unit i, and nodal points of bars belonging to units $i-2$, $i-1$, $i+1$, and $i+2$. Note that the number of tendons is not minimal for the structure to be self-stressable [21]. For instance, all diagonal tendons $t_{4,5,8,9}^i$ can be removed, while the structure still has integrity and does not become a mechanism.

The left side of the structure has to be modified, and is given in Fig. 2. Besides modification for the differences in boundary geometry, the left side removes the three degrees-of-freedom of the rigid body; in effect, it restricts movement of the upper left node in both x and y-coordinate direction, i.e., the node is translationally fixed, and of the lower left node in the x-direction. A result of the fixations is that the vertical left tendon t_1^1 of the structure cannot rotate, although both bars of unit $i = 1$ are still free to rotate. Note that tendons t_{6-9}^i no longer appear for $i = 1$ and that some tendons connect to other nodes than in the previous figure.

The right side is in Fig. 3. No nodes are fixed at this boundary. Only differences in geometry are taken into account, the connection of some tendons is to different nodes than in Fig. 1.

III. Tensegrity Structure Model

Two models are developed, a nonlinear model for arbitrary displacements and a linearized model, valid for small displacements only, for use in a linear plant model. The nonlinear model can be used to evaluate the results with simulations, and to access robustness issues.

The basic assumptions in setting up the nonlinear model are the following:

1) a bar is straight and of uniform cross section and density;
2) the central moment of inertia of a bar for rotation around its principle axis is zero;

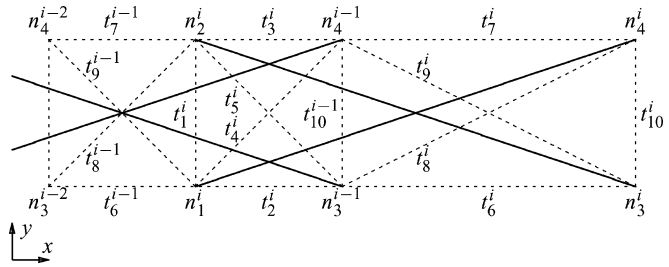

Fig. 3. Right unit of planar tensegrity structure $i = n$.

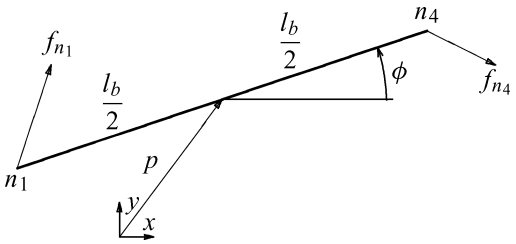

Fig. 4. Elementary bar in planar tensegrity structure.

3) a bar is of fixed length, so infinitely stiff axially;
4) a tendon is massless;
5) a tendon has no torsional or bending stiffness, but axial stiffness;
6) a bar has two nodal points, which are of zero dimension;
7) a tendon is connected to a bar at a nodal point only;
8) external loads are only applied at a nodal point;
9) external loads do not include bending or torsional loads on members;
10) there are no potential fields (e.g., gravity).

Due to these assumptions, the bars are axially loaded only, except during transients, but we neglect this effect. Although members in a tensegrity structure are axially loaded only, the structure itself has a finite stiffness for bending and torsion.

The model of the complete structure is quite elementary, being built up of bars that are connected by elastic tendons, and can best be developed by a classical Newtonian formulation, because we are also interested in forces internal to the structure.

The model for a single bar, see Fig. 4, moving in the plane is

$$m\ddot{p} = F_b$$
$$J\ddot{\phi} = M_b$$

using as the three generalized coordinates the position p of the center of mass and the orientation angle ϕ around this center. The mass m and the central moment of inertia J are the physical parameters that specify the dynamics of a bar. The force F_b and the moment M_b depend on the forces exerted by the tendons connected to the nodes of the bar, and therefore depend on the position of nodal points and the unstressed length of tendons that are modeled as unidirectional springs.

We compute the forces F_b and moment M_b from the nodal force vectors f_{n_1} and f_{n_4}, assumed given in Cartesian components, by

$$F_b = f_{n_1} + f_{n_4}$$
$$M_b = \frac{l_b}{2}[\sin\phi \quad -\cos\phi]f_{n_1} + \frac{l_b}{2}[-\sin\phi \quad \cos\phi]f_{n_4}.$$

Nodal forces f_n are computed by summing tendon forces f_t for those tendons connected to a particular node, taking account of a sign convention, $f_n = \sum \pm f_t$. If there is a disturbance force w_n acting on the nodes we get

$$f_n = \sum \pm f_t + w_n.$$

The bookkeeping needed to know over which tendons to sum and which sign to use is not detailed. For a systematic way to do that, see [22] and [23]. The direction of the tendon force vector f_t comes from the tendon vector t because those vectors are aligned

$$f_t = \frac{F}{l}t$$

where the tendon vector needs to be scaled by its length $l = ||t||$.

To compute the tendon force magnitude F we need constitutive equations. The model for a tendon is derived from classical continuum mechanics, with linear elastic material behavior, so $\sigma = E\varepsilon$ with E the modulus of elasticity, and where $\sigma = F/A$, the stress, is the ratio of force and cross-sectional area, and $\varepsilon = \Delta l/l_0$, the strain, is the elongation $\Delta l = l - l_0$ divided by the unstressed length l_0. This gives

$$F = \frac{EA}{l_0}(l - l_0) = k_t(l - l_0)$$

which is used to compute the force magnitude F given l_0 and l. When the tendon control input u_t changes the tendon rest-length, we have to use

$$F = k_t(l - l_0 + u_t).$$

To compute the unstressed length when both F and l are known, $l_0 = l/(1 + (F/EA))$ is used. We need this only to establish initial conditions corresponding to a static equilibrium.

A tendon vector t is computed as the difference of the two nodal point vectors that the tendon connects to

$$t = p_{n_j} - p_{n_k}$$

while the Cartesian coordinates p_n of the nodal points can be computed as

$$p_{n_1} = p - \frac{l_b}{2}\begin{bmatrix}\cos\phi\\ \sin\phi\end{bmatrix}, \quad p_{n_4} = p + \frac{l_b}{2}\begin{bmatrix}\cos\phi\\ \sin\phi\end{bmatrix}.$$

By following this sequence of formulas backward, we can, given p and ϕ of all bars, compute F_b and M_b for all bars. The equations for individual bars can be taken together to form the following set of differential equations, taking account also of the boundary conditions:

$$M\ddot{q} = T(q, w, u) - D\dot{q}$$
$$q^T = [p_{1x} \quad p_{1y} \quad \phi_1 \quad \dots \quad \phi_{2n}]$$

where q gathers the positions p and orientations ϕ, the generalized force T gathers the forces F_b and moments M_b, the load w gathers w_n, and the control input u gathers the u_t. In these equations, damping proportional to the speed $\dot{q}$ has been incorporated, with D a diagonal matrix of nonnegative damping factors. For a static model $\ddot{q}$ and $\dot{q}$ are equated to zero and the resulting algebraic equations, $T(q, w, u) = 0$, represent the equilibrium

conditions. Outputs of the model are performance variables z and measurements y.

Combining all this we can formulate the following sets of equations:

$$\begin{aligned}\dot{x} &= f(x, v, u)\\ z &= g(x, v, u)\\ y &= h(x, v, u)\end{aligned}$$

with

$$x = \begin{bmatrix} q \\ \dot{q} \end{bmatrix}.$$

Here, v includes the loads w, but also other exogenous signals like measurement noise.

Due to self-stressability, the stability of the system is determined by the operating conditions, e.g., multiple equilibria [24] with snap-through transitions [25] may occur. In the sequel, we consider operating conditions that generate an equilibrium that is asymptotically stable (if $D > 0$).

IV. Linearized Control Model

For design of a controller a linear model is beneficial. Experimental data [5], [15], [26] suggests that a linear approximation is valid locally, as long as the joints are ideal, i.e., do not deform nonlinearly and have no friction, and the structure is self-stressed sufficiently to avoid play in the joints and tendons going slack.

The linear model is derived directly by numerical differentiation of the nonlinear model in state–space form. This is possible, because no nonsmooth terms, e.g., due to friction or hysteresis, are present in the model. For this linear model, where the variables x, v, u, z, and y now denote variations around their equilibrium values, we write

$$\begin{aligned}\dot{x} &= Ax + B_v v + B_u u\\ z &= C_z x + D_{zv} v + D_{zu} u\\ y &= C_y x + D_{yv} v + D_{yu} u\end{aligned}$$

with u a set of control inputs, i.e., the actuators to be selected, v a set of exogenous inputs, y a set of measurements, i.e., the sensors to be selected, and z a set of to-be-controlled variables. The exogenous inputs are external loads at, or displacements of, designated nodes w_n or p_n and sensor measurement noise. The to-be-controlled variables are displacements or accelerations of designated nodes p_n or $\ddot{p}_n$ and control inputs u. The matrices involved in the model follow from the Jacobians of f, g, and h.

The linear model can be formulated in the Laplace domain as

$$\begin{bmatrix} z \\ y \end{bmatrix} = P(s) \begin{bmatrix} v \\ u \end{bmatrix}$$

where P denotes the plant model.

The standard plant setup, using four types of signals (exogenous signals, controller signals, to-be-controlled variables, and measured signals), is selected for our purposes because it is general and embraces a lot of control problems, like set-point regulation, tracking, and disturbance rejection.

As is usual, performance specifications are characterized by choosing shaping functions V for v and weighting functions Z for z. These functions allow to characterize the real, for v, or desired, for z, frequency contents of the signals, and make it possible to express the relative importance of the signals.

A controller C will be used to close the loop around P and generate the closed-loop system H. In a norm based controller design, the controller C is designed so the weighted closed-loop ZHV will have a system norm equal to or below a performance bound γ, if that is feasible. Feasibility depends, among others, on the set of actuators and sensors employed.

V. $\mathcal{H}_\infty$ Controller Conditions and Feasibility

We address the selection of actuating/sensing tendons that are needed to achieve a desired level of closed-loop performance. The selection of IO sets with guaranteed performance is based on existence conditions for stabilizing controllers that achieve a specified $\mathcal{H}_\infty$ performance bound γ. It is not necessary to design a controller and than check the properties of the closed loop, which would be time consuming.

$\mathcal{H}_\infty$-techniques have the advantages of a sound theoretical foundation, of readily available analysis and synthesis software, and of necessary and sufficient existence conditions. The feasibility test consists of checking the conditions for the existence of a stabilizing $\mathcal{H}_\infty$ controller achieving the specified performance level γ. Efficient tools for this task are available and may be based on Riccati equations [27] or on conditions expressed in terms of LMI [28], [29]. As in [20], we employ a Riccati-equation based technique, being more efficient.

Then, for feasibility the following properties are sequentially checked:

- stabilizability of (A, B_u);
- detectability of (A, C_y);
- norm of the minimal direct feedthrough;
- conditions on the input Hamiltonian, used to solve the control Riccati equation;
- conditions on the output Hamiltonian, for the filter Riccati equation;
- spectral radius condition.

The feasibility test consists of several necessary conditions, that together are sufficient. This leads itself naturally to a streamlined computation. If one of the necessary conditions is not fulfilled, the remaining conditions do not need to be checked. So only for feasible combinations are all checks done. Further efficiency can be obtained due to the structure of the individual conditions. For instance, stabilizability and detectability need not be checked at all if the open loop is stable.

VI. IO Selection Approach

Our goal is to characterize the full set of feasible solutions, i.e., combinations of actuators and sensors for which a controller exists that can guarantee the desired level of performance for the closed-loop system. To select combinations of inputs and outputs (also called IO sets), we need two things: an algorithm to efficiently search for promising combinations and a feasibility test that assesses a single candidate IO set. The feasibility test should be efficient because it is called often. The test we employ should tell something about control relevant performance. A way to circumvent time-consuming steps in the feasibility test

was discussed in the previous section. How to tame the combinatorially explosive search is discussed now.

The search is based on an algorithm to generate all maximal independent or all minimal dependent sets, defined in the following. The algorithm was proposed in [30] and implemented in [31]. We briefly explain the problem setup and the usefulness of the algorithm to make the exposition self-contained.

Let E be the finite set of all actuators and sensors that are considered, with cardinality $|E| = n$, and let $\mathcal{I}$ be a nonempty family of subsets of E that satisfies the following rule: if $I \in \mathcal{I}$ and $I' \subseteq I$ then $I' \in \mathcal{I}$. Now, $(E, \mathcal{I})$ is called an independence system and $\mathcal{I}$ is its family of independent sets. An independent set I is called maximal if there is no $I' \in \mathcal{I}$ such that $I' \supset I$. Subsets of E that are not in $\mathcal{I}$ are dependent sets. All dependent sets form the family $\mathcal{J}$. A dependent set J is minimal if $J' \in \mathcal{I}$ for all $J' \subset J$.

The IO selection problem with a monotonous selection criterion exactly fits an independence system problem. A monotonous selection criterion is one where the performance does not deteriorate when an IO set is expanded with additional devices. The family of subsets $\mathcal{I}$ gathers all actuator/sensor combinations that are not acceptable and $\mathcal{J}$ gathers all acceptable ones.

Now the problem is to establish the structure of the independence system, i.e., to find $\mathcal{I}$ and/or $\mathcal{J}$. To do this, an oracle is available that decides whether a subset of E belongs to $\mathcal{I}$ or $\mathcal{J}$. In general, it suffices to find the K maximal independent sets of $\mathcal{I}$ or the M minimal dependent sets of $\mathcal{J}$, because with these sets one can generate the families $\mathcal{I}$ and/or $\mathcal{J}$ without visiting the oracle. Because both K and M are bounded by $\binom{n}{n/2}$, one cannot expect to obtain a solution in time polynomial in n. One may wonder if a solution for finding $\mathcal{I}$ or $\mathcal{J}$ in time polynomial in n and K or M is possible. Lawler *et al.* [32] state that the problem of finding the K maximal independent or M minimal dependent sets is $\mathcal{NP}$-hard and there is no solution possible in time polynomial in n, K, and M. However, in [30], it is shown to be possible to establish all K maximal independent sets and all M minimal dependent sets visiting the oracle only $O(nK+M)$ or $O(K+nM)$ times, using a depth-first search. This means that a complete solution with visits affine in n, K, and M is possible. An algorithm that achieves this has been used.

When the number n of possible devices is large, the number of feasibility tests is also large, because in general M and K will be large, except in those cases where either a very small or a very large fraction of the devices is needed to meet the performance level. In general, when n exceeds the range 32 to 40 one needs to consider alternative strategies. A possible heuristic is to extract from separate input and output selection, with a smaller number of devices for each, those devices that are most promising, e.g., by selecting those that:

- occur often in minimal dependent sets;
- occur in minimal dependent sets with a low number of devices;
- occur in maximal independent sets with a low number of devices;
- do not occur in maximal independent sets with a large number of devices.

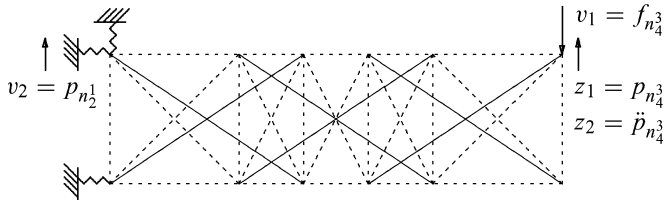

Fig. 5. Three-unit planar tensegrity structure. Bars: ——. Tendons: – –.

By eliminating devices that are not expected to add much, the size of the problem is reduced and a combined selection is tractable. The application section gives examples of the use of these heuristic rules.

VII. Application

The approach is illustrated for a three-unit planar tensegrity model with six bars and twenty-six tendons, see Fig. 5, but can be used for other selection problems. We therefore have twenty-six potential actuators and twenty-six potential sensors, so $n = 52$ potential input–output devices, making $\approx 2^{52}$ or $\approx 4.5 \cdot 10^{15}$ unique combinations possible. This is much larger than any other application of rigorous procedures considered before. Note from Fig. 5 that in this application the rigid support is replaced by a flexible one, using one-directional stiff springs, to make the problem more realistic and to make it straightforward to use both displacement and force disturbances.

Two typical design specifications are explored, as indicated in Fig. 5. The first case is to stiffen a planar tensegrity structure, shaped like a cantilever beam, for dynamic external loading. Here, v_1 represents a vertical load on the right/top node and z contains the corresponding nodal deflection z_1, together with the control inputs u, included to limit the control expenditure. The second case is to dampen vibrations when the structure is considered as an erected building loaded by ground excitations. Here, v_2 represents a vertical displacement of the foundation at the top/left node and z contains the vertical acceleration of the top/right node z_2, besides the control inputs u. For both cases, actuators adjust the rest-length l_0 of a tendon and sensors deliver the length l of a tendon. For Case 2 we emphasize higher frequencies more than for Case 1, due to the use of acceleration instead of displacement.

To simplify matters, the weighting functions V and Z are chosen to be static weights. Now, the number of states of the generalized plant is not that large, namely 36, to speed up computations. The static weights are chosen so all weighted signals (measurement noise, external force or displacement, control input, displacement or acceleration) have an appreciable influence on the achievable $\mathcal{H}_\infty$-norm. This implies that none of the components is over-specified, so the selection is cost-effective.

Actuator noise can cause a violation of the monotonicity assumption shown previously. To use the independence system setup, noise present in the input signal u should vanish if the signal's amplitude is zero. Hence, the actuators are noiseless in the application. There is no need to check stabilizability and detectability in this case, because both the plant P and the functions V and Z are asymptotically stable, and so is their serial connection, the open-loop system.

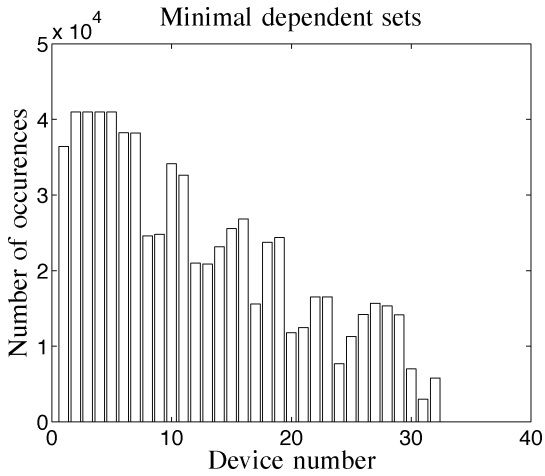

Fig. 6. Results for minimal dependent IO sets for $\gamma = 0.3$.

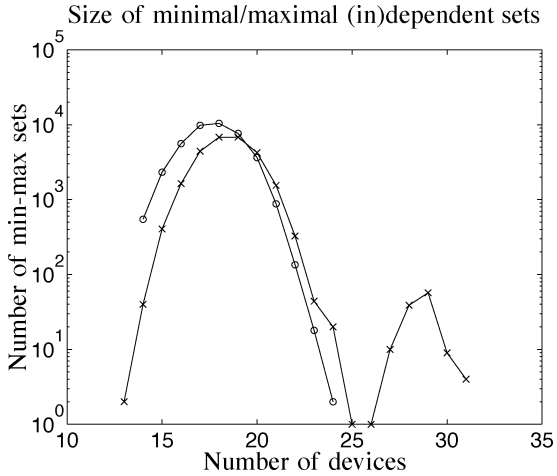

Fig. 7. Number of devices for $\gamma = 0.3$. "o": minimal dependent, "x": maximal independent IO sets.

A. Case 1: Dynamic Stiffness Improvement

For the full IO set the achievable value of the $\mathcal{H}_\infty$-norm is slightly smaller than $\gamma = 0.3$. For a required performance level of $\gamma = 0.3$, IO selection has been carried out for a subset of 16 from the 26 tendons, so $n = 32$, and the number of actuators and sensors in the base set is equal and allows collocation. The tendons selected were those that during separate input and output selection often yielded promising actuators or sensors. To present the results a representation is chosen that only sums the number of occurrences of a device in the minimal dependent sets. Fig. 6 compactly represents the 40 960 minimal dependent sets that completely characterize the feasible and infeasible IO sets. There are four devices (2–5) that are always needed. Note that more actuators (devices numbered 1–16) than sensors (devices numbered 17–32) are needed, so not only collocated devices are selected.

Another way to present the results is by showing how many devices are in the minimal dependent or maximal independent sets. This information is in Fig. 7. The smallest feasible IO set has 14 devices, and there are 545 of these sets, mostly permutations of a slightly larger number of devices, but the number of these sets is inconveniently large. The most convenient information is available from the data for the maximal independent

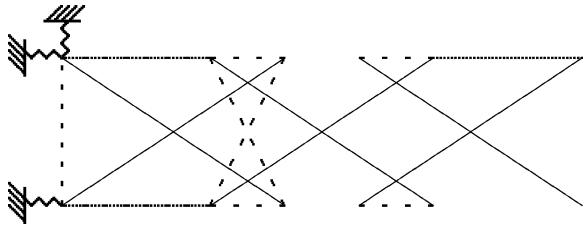

Fig. 8. Most profitable devices for Case 1. Actuators: — —. Sensors: · · ·.

IO sets. Two of those sets have 13 devices and adding any of the remaining 19 devices makes them feasible, so the devices in those two sets are ranked high. There are four maximal independent sets of size $n-1$, which implies that four of the devices appear in all minimal dependent sets, because they are always needed, and therefore rank high. This agrees with Fig. 6. A similar reasoning will prefer devices that are not included in the nine maximal independent sets of size $n-2$. In this way, also the most promising devices in separate input and output selection were chosen.

The most profitable IO devices are indicated in Fig. 8. Not all of them are collocated ones. A physical interpretation of the results indicates that horizontal tendons, those "perpendicular" to the disturbance, are preferred, both for actuation and sensing. Furthermore, actuators close to the support are preferred, because they provide a higher leverage. Note that no vertical inner tendons are used.

B. Case 2: Vibration Reduction

For the full IO set the achievable value of the $\mathcal{H}_\infty$-norm is slightly smaller than 1, namely $\gamma = 0.9849$. For this case we first present results for actuator selection (so $n = 26$) that show how the search for the minimal dependent or maximal independent sets is accomplished. For a performance level $\gamma = 5$, M and K are rather small, permitting a presentation of those results (Figs. 9 and 10). The main purpose is to show how the search direction influences the number of feasibility tests to be performed.

Fig. 9 presents results for finding minimal dependent sets, using a top-down search direction. The figure illustrates the depth first search. Starting from the top (with $l = n = 26$), devices from the full IO set are eliminated, until no further elimination is possible without becoming infeasible. Then another base IO set is chosen, with $l = n - 1$ devices or with another permutation of devices, and the elimination starts again, until for all 2^{26} possible IO sets it is clear whether they are feasible or not. Each vertical sequence is, thus, a trace of evaluated IO sets which ends in finding a minimal dependent set. For this case the number of evaluations is 815 and $M = 108$.

Fig. 10 presents results for finding maximal independent sets, employing a bottom-up search direction. Here we start with the empty IO set (the open loop), which is not feasible, and add devices until no device can be added without the resulting IO set becoming feasible. The number of evaluations is 348 and $K = 31$, so this search direction needs less evaluations. The test is also more efficient, encountering more infeasible sets.

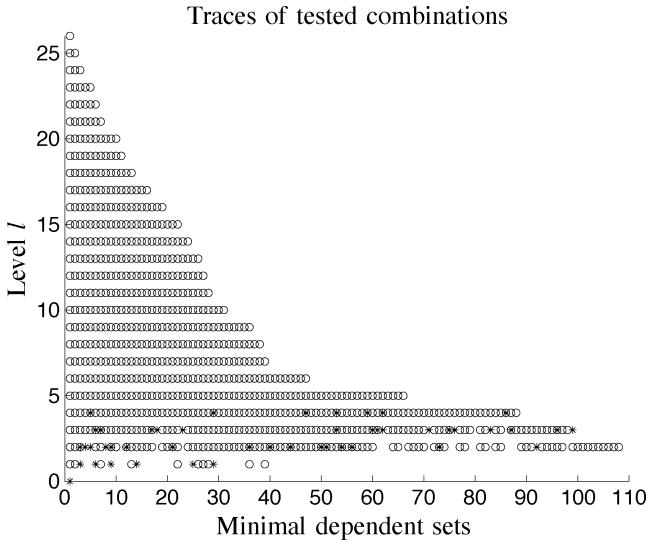

Fig. 9. Search for minimal dependent inputs sets for $\gamma = 5$. "o": feasible ones. "x": infeasible ones.

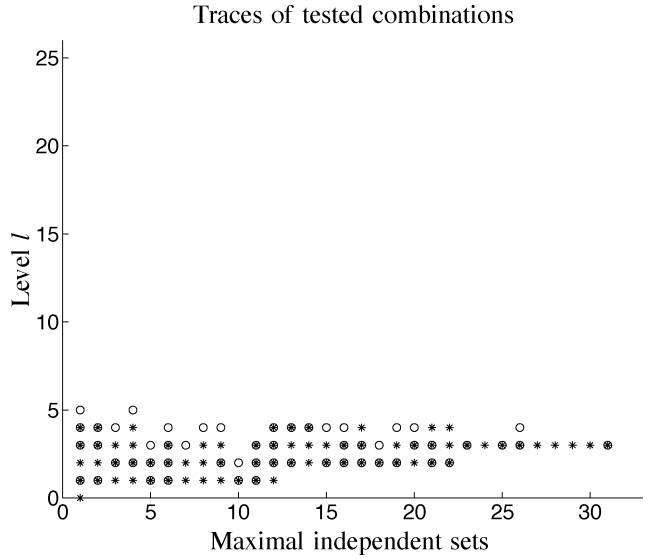

Fig. 10. Search for maximal independent input sets for $\gamma = 5$. "o": feasible ones. "x": infeasible ones.

The combinatorial part of the search is in guaranteeing that IO sets are not evaluated when from the available results it is clear that they are feasible or infeasible. Details of how this can be done efficiently are in [31]. This part is easier for small values of K and M. In general, K and M are relatively small when either the specs are very tight (needing almost any device) or very loose (only a few devices are needed). Here the specifications are loose, because $\gamma = 5$ is relatively large.

Combining the most promising actuators with similar results for sensor selection gives a selection problem with 8 input and 24 output devices, so $n = 32$. In this case, we do not use an equal number of actuators and sensors in the base set, because more sensors are needed than actuators to achieve a desired level of performance, as will become clear from the results presented. The selection is solved for $\gamma = 1$, so only slightly worse than

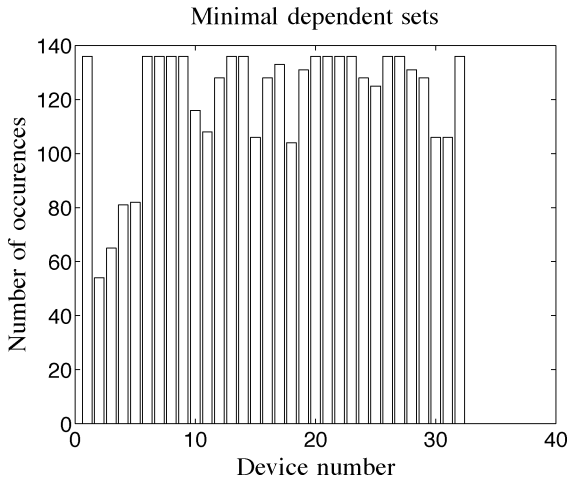

Fig. 11. Results for minimal dependent IO sets for $\gamma = 1$.

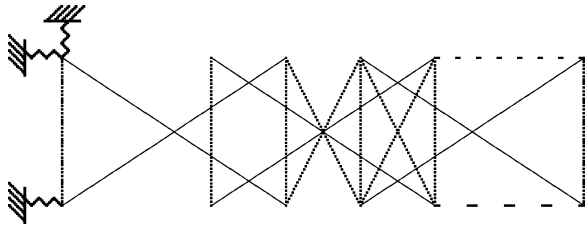

Fig. 12. Most profitable devices for Case 2. Actuators: — —. Sensors: · · ·.

achievable with the full set of devices. The most promising devices are indicated with large bars in Fig. 11, because they appear in all 136 minimal dependent sets. The 8 actuators have device numbers 1–8. Note that the number of sensors needed is much larger than the number of actuators. It shows that a requirement for actuators and sensors to appear as collocated pairs would require a larger number of devices to achieve the same performance.

Some of the most profitable devices are shown in Fig. 12. A physical interpretation of the results indicates that actuators and sensors connected and "parallel" to the disturbance are preferred. Furthermore, there is a tendency for the actuators to be concentrated close to the performance output, having less structural mass to displace, and for the sensors to be concentrated in the middle, with an orientation parallel to the disturbance and the performance output.

Note that these results differ from the results for the other case, especially with respect to the horizontal (Case 1) and vertical (Case 2) preferred orientation. With the different goals targeted by the control specifications, this is not surprising.

Given the straightforward physical interpretation of the results, we do not expect a search based on all 52 devices to give results that are significantly different from the results obtained by first selecting inputs and outputs separately, followed by a combined IO selection.

VIII. Conclusion

An efficient and rigorous procedure for input–output selection was shown to be readily applicable to tensegrity structures

with a large number of potential IO sets due to the use of an additional heuristic.

The trend in the results suggests, for vibration reduction problems, one should choose sensors in strings parallel to the disturbance vector, whereas, for dynamic stiffness improvement, the best sensor strings are perpendicular to the disturbance vector. The same holds for actuators. For vibration suppression the number of sensors needed was larger than the number of actuators, while the reverse was true for dynamic stiffness improvement. This shows that the set of feasible solutions depends on the goal of the controlled system.

The results are also beneficial when making choices in the design of tensegrity systems, because they indicate which tendons are needed and which can be eliminated when there is some redundancy in the tendons, i.e., in case not all of the original tendons are needed to guarantee self-stressability.

REFERENCES

[1] R. E. Skelton, "Structural systems: a marriage of structural engineering and system science," *J. Struct. Control*, vol. 9, no. 2, pp. 113–133, Aug. 2002.

[2] R. Motro and V. Raducanu, "Tensegrity systems," *Int. J. Space Structures*, vol. 18, no. 2, pp. 77–84, May 2003.

[3] H. Klimke, S. Stephan, and R. Essrich, "Fertigung und Montage des Messeturms in Rostock," *Stahlbau*, vol. 73, no. 2, pp. 74–79, Feb. 2004.

[4] D. E. Ingber, "Tensegrity I. Cell structure and hierarchical systems biology," *J. Cell Sci.*, vol. 116, no. 7, pp. 1157–1173, Apr. 2003.

[5] E. Fest, K. Shea, and I. F. C. Smith, "Active tensegrity structures," *J. Struct. Eng.*, vol. 130, no. 10, pp. 1454–1465, Oct. 2004.

[6] J. T. Scruggs and W. D. Iwan, "Control of a civil structure using an electric machine with semiactive capability," *J. Struct. Eng.*, vol. 129, no. 7, pp. 951–959, Jul. 2003.

[7] A. G. Tibert and S. Pellegrino, "Deployable tensegrity reflectors for small satellites," *J. Spacecraft Rockets*, vol. 39, no. 5, pp. 701–709, Sep.–Oct. 2002.

[8] C. Sultan and R. Skelton, "Deployment of tensegrity structures," *Int. J. Solids Structures*, vol. 40, no. 18, pp. 4637–4657, Sep. 2003.

[9] M. van de Wal and B. de Jager, "A review of methods for input/output selection," *Automatica—J. IFAC*, vol. 37, no. 4, pp. 487–510, Apr. 2001.

[10] A. Chattopadhyay and C. E. Seeley, "A simulated annealing technique for multiobjective optimization of intelligent structures," *Smart Mater. Struct.*, vol. 3, no. 2, pp. 98–106, Jun. 1994.

[11] M. Sener, S. Utku, and B. K. Wada, "Geometry control in prestressed adaptive space trusses," *Smart Mater. Struct.*, vol. 3, no. 2, pp. 219–225, Jun. 1994.

[12] H. S. Tzou and J. J. Hollkamp, "Collocated independent modal control with self-sensing orthogonal piezoelectric actuators (theory and experiment)," *Smart Mater. Struct.*, vol. 3, no. 3, pp. 277–284, Sep. 1994.

[13] E. Tongco and D. Meldrum, "Optimal sensor placement of large flexible space structures," *J. Guid. Control Dyn.*, vol. 19, no. 4, pp. 961–963, Jul.–Aug. 1996.

[14] X. Liu, D. W. Begg, and D. R. Matravers, "Optimal topology/actuator placement design of structures using SA," *J. Aerospace Eng.*, vol. 10, no. 3, pp. 119–125, Jul. 1997.

[15] G. J. Balas and P. M. Young, "Sensor selection via closed-loop control objectives," *IEEE Trans. Contr. Syst. Technol.*, vol. 7, no. 6, pp. 692–705, Nov. 1999.

[16] R. K. Kincaid and S. L. Padula, "D-optimal designs for sensor and actuator locations," *Comput. Oper. Res.*, vol. 29, no. 6, pp. 701–713, May 2002.

[17] Y. J. Yan and L. H. Yam, "Optimal design of number and locations of actuators in active vibration control of a space truss," *Smart Mater. Struct.*, vol. 11, no. 4, pp. 496–503, Aug. 2002.

[18] C. J. Damaren, "Optimal location of collocated piezo-actuator/sensor combinations in spacecraft box structures," *Smart Mater. Struct.*, vol. 12, no. 3, pp. 494–499, Jun. 2003.

[19] Q. S. Li, D. K. Liu, J. Tang, N. Zhang, and C. M. Tam, "Combinatorial optimal design of number and positions of actuators in actively controlled structures using genetic algorithms," *J. Sound Vib.*, vol. 270, no. 4–5, pp. 611–624, Mar. 2004.

[20] B. de Jager and M. van de Wal, "Efficient selection of inputs and outputs for robust control," in *Proc. 38th IEEE Conf. Decision and Control*, Phoenix, AZ, Dec. 1999, pp. 4517–4522.

[21] A. Hanaor, "Prestressed pin-jointed structures-flexibility analysis and prestress design," *Comput. Struct.*, vol. 28, no. 6, pp. 757–769, 1988.

[22] H.-J. Schek, "The force density method for form finding and computation of general networks," *Comput. Methods Appl. Mech. Engrg.*, vol. 3, no. 1, pp. 115–134, Jan. 1974.

[23] D. Williamson, R. E. Skelton, and J. Han, "Equilibrium conditions of a tensegrity structure," *Int. J. Solids Structures*, vol. 40, no. 23, pp. 6347–6367, Nov. 2003.

[24] M. Defossez, "Shape memory effects in tensegrity structures," *Mech. Res. Comm.*, vol. 30, no. 4, pp. 311–316, Jul.–Aug. 2003.

[25] M. R. Sheidaii, G. A. R. Parke, K. Abedi, and A. Behravesh, "Dynamic snap-through buckling of truss-type structures," *Int. J. Space Structures*, vol. 16, no. 2, pp. 85–93, Jun. 2001.

[26] M. Salama, J. Umland, R. Bruno, and J. Garba, "Shape adjustment of precision truss structures: analytical and experimental validation," *Smart Mater. Struct.*, vol. 2, no. 4, pp. 240–248, Dec. 1993.

[27] K. Glover and J. C. Doyle, "State-space formulae for all stabilizing controllers that satisfy an H_∞ norm bound and relations to risk sensitivity," *Syst. Control Lett.*, vol. 11, no. 3, pp. 167–172, Sep. 1988.

[28] P. Gahinet and P. Apkarian, "A linear matrix inequality approach to $\mathcal{H}_\infty$ control," *Int. J. Robust Nonlinear Control*, vol. 4, no. 1, pp. 421–448, Jan.–Feb. 1994.

[29] T. Iwasaki and R. E. Skelton, "All controllers for the general $\mathcal{H}_\infty$ control problem: LMI existence conditions and state space formula," *Automatica—J. IFAC*, vol. 30, no. 8, pp. 1307–1317, Aug. 1994.

[30] B. de Jager and O. Toker, "Complexity of input output selection," in *Proc. Int. Symp. Mathematical Theory of Networks and Systems (MTNS'98)*, Padova, Jul. 1998, pp. 597–600.

[31] B. de Jager and J. Banens, "VISOR: vast independence system optimization routine," *Algorithmica*, vol. 30, no. 4, pp. 630–644, 2001.

[32] E. L. Lawler, J. K. Lenstra, and A. H. G. Rinnooy Kan, "Generating all maximal independent sets: NP-hardness and polynomial-time algorithms," *SIAM J. Comput.*, vol. 9, no. 2, pp. 558–565, Aug. 1980.